Role of random electric fields in relaxors

Daniel Phelan[a], Christopher Stock[a,b], Jose A. Rodriguez-Rivera[a,c], Songxue Chi[a,c], Juscelino Leão[a], Xifa Long[d], Yujuan Xie[d], Alexei A. Bokov[d], Zuo-Guang Ye[d], Panchapakesan Ganesh[e], and Peter M. Gehring[a,1]

[a]NIST Center for Neutron Research, National Institute of Standards and Technology, Gaithersburg, MD 20899; [b]School of Physics and Astronomy, University of Edinburgh, Edinburgh EH9 3JZ, United Kingdom; [c]Department of Materials Science and Engineering, University of Maryland, College Park, MD 20742; [d]Department of Chemistry and 4D LABS, Simon Fraser University, Burnaby, BC, Canada V5A 1S6; and [e]Center for Nanophase Materials Sciences, Oak Ridge National Laboratory, Oak Ridge, TN 37831-6494

Edited by Alexis T. Bell, University of California, Berkeley, CA, and approved December 24, 2013 (received for review August 4, 2013)

$PbZr_{1-x}Ti_xO_3$ (PZT) and $Pb(Mg_{1/3}Nb_{2/3})_{1-x}Ti_xO_3$ (PMN-*x*PT) are complex lead-oxide perovskites that display exceptional piezoelectric properties for pseudorhombohedral compositions near a tetragonal phase boundary. In PZT these compositions are ferroelectrics, but in PMN-*x*PT they are relaxors because the dielectric permittivity is frequency dependent and exhibits non-Arrhenius behavior. We show that the nanoscale structure unique to PMN-*x*PT and other lead-oxide perovskite relaxors is absent in PZT and correlates with a greater than 100% enhancement of the longitudinal piezoelectric coefficient in PMN-*x*PT relative to that in PZT. By comparing dielectric, structural, lattice dynamical, and piezoelectric measurements on PZT and PMN-*x*PT, two nearly identical compounds that represent weak and strong random electric field limits, we show that quenched (static) random fields establish the relaxor phase and identify the order parameter.

lead zirconate titanate | piezoelectricity | short-range order | soft modes | neutron scattering

The remarkable electromechanical properties of lead-oxide perovskite (ABO_3) relaxors such as $Pb(Mg_{1/3}Nb_{2/3})_{1-x}Ti_xO_3$ (PMN-*x*PT) and $Pb(Zn_{1/3}Nb_{2/3})_{1-x}Ti_xO_3$ (PZN-*x*PT) have inspired numerous attempts to understand the piezoelectricity in terms of the structural phase diagram, which contains a steep morphotropic phase boundary (MPB) separating pseudorhombohedral and tetragonal states over a narrow compositional range where the piezoelectricity is maximal (1–5). These materials exhibit very low strain–electric field hysteresis, extremely large dielectric constants, and record-setting piezoelectric coefficients at room temperature that form an unusually appealing set of properties with the potential to revolutionize a myriad of important technological applications spanning medical diagnostic sonography, military sonar, energy harvesting, and high-precision actuators (6–8). Many researchers have argued that quenched random electric fields (REFs) play a central role in establishing the relaxor phase, in part because the *B* sites of all known lead-oxide perovskite relaxors are occupied by random mixtures of heterovalent cations (9–13). However, there is ample theoretical work that suggests relaxor behavior can occur in the absence of REFs (14–16). In fact it has not been proven conclusively that REFs are essential to the relaxor state or that they play any role in the ultrahigh piezoelectricity. These basic questions persist in the face of decades of research mainly because there exists no rigorous definition of what a relaxor is, i.e., there is no precise mathematical formulation of the relaxor-order parameter. To date, any material for which the real part of the dielectric permittivity $\epsilon'(\omega, T)$ exhibits a broad peak at a temperature T_{max} that depends strongly (and in some cases only weakly) on the measuring frequency, ω, is classified as a relaxor. This definition has been applied equally to PMN and PZN, which possess strong REFs, as well as to specific compositions of $K(Ta_{1-x}Nb_x)O_3$, $(K_{1-x}Li_x)TiO_3$, $Ba(Zr_{1-x}Ti_x)O_3$ (BZT), and $Ba(Sn_{1-x}Ti_x)O_3$ (BST) (17, 18), which are all composed of homovalent cations and thus have much weaker REFs. The REFs in these latter materials are believed to result (primarily) from cation off-centering and are nonzero when this off-centering is static. We will use the term "weak REF limit" to make clear that the REFs in such materials are not necessarily zero.

To identify REF-specific properties one must compare identical systems that differ only in the strength of the REFs. Although such an idealized situation does not exist, the recent breakthrough in the growth of millimeter-size, high-quality single crystals of $Pb(Zr_{1-x}Ti_x)O_3$ (PZT) (19) has finally provided experimentalists with a nearly perfect model system with which such a comparison can be made to classic relaxor systems such as PMN-*x*PT. Both PZT and PMN-*x*PT are chemically disordered, lead-oxide perovskites, and both exhibit similar phase diagrams as a function of Ti concentration that contain an MPB near which exceedingly large piezoelectric coefficients are observed. Moreover, both materials possess nearly identical average *B*-site ionic radii; the average *B*-site ionic radius of PMN is equal to that of PZT with a composition of 46% Ti. However, whereas PMN possesses strong REFs, PZT is composed of homovalent Zr^{4+} and Ti^{4+} *B*-site cations and is thus representative of the weak REF limit. In this article we present a combination of dielectric permittivity, piezoelectric, and neutron scattering measurements on each material that indicate that strong REFs are necessary to the formation of the relaxor phase in lead-oxide perovskites and greatly amplify the piezoelectric response. We develop a heuristic model to motivate the order parameter associated with the relaxor phase that suggests a modified definition of relaxors.

Fig. 1*A* illustrates how the real part of the dielectric permittivity of PMN varies with temperature at four different measuring frequencies. From 10^2 to 10^5 Hz, the position of the maximum dielectric permittivity shifts to higher temperature by 18 K; this behavior is the hallmark of all relaxors. By contrast, the same measurement made over the same frequency range on a single crystal specimen of PZT with $x = 0.325$ is

Significance

Relaxors are characterized by a frequency-dependent peak in the dielectric permittivity and are critical to modern technological applications because they exhibit large dielectric constants and unparalleled piezoelectric coefficients. Despite decades of study a fundamental understanding of the origin of relaxor behavior is lacking. Here we compare the structural, dynamical, dielectric, and piezoelectric properties of two highly similar piezoelectric lead-oxide materials: ferroelectric $PbZr_{1-x}Ti_xO_3$ and relaxor $Pb(Mg_{1/3}Nb_{2/3})_{1-x}Ti_xO_3$. Random electric fields are implicated as the genesis of relaxor behavior, and the diffuse scattering associated with short-range polar order is identified as the order parameter. The piezoelectric response is found to be greatly amplified in crystals that display this diffuse scattering.

Author contributions: D.P., C.S., X.L., Y.X., A.A.B., Z.-G.Y., P.G., and P.M.G. designed research; D.P., C.S., J.A.R.-R., S.C., X.L., Y.X., A.A.B., Z.-G.Y., P.G., and P.M.G. performed research; J.B.L., X.L., Y.X., and Z.-G.Y. contributed new reagents/analytic tools; D.P., C.S., and J.A.R.-R. analyzed data; and D.P. and P.M.G. wrote the paper.

The authors declare no conflict of interest.

This article is a PNAS Direct Submission.

[1]To whom correspondence should be addressed. E-mail: peter.gehring@nist.gov.

This article contains supporting information online at www.pnas.org/lookup/suppl/doi:10.1073/pnas.1314780111/-/DCSupplemental.

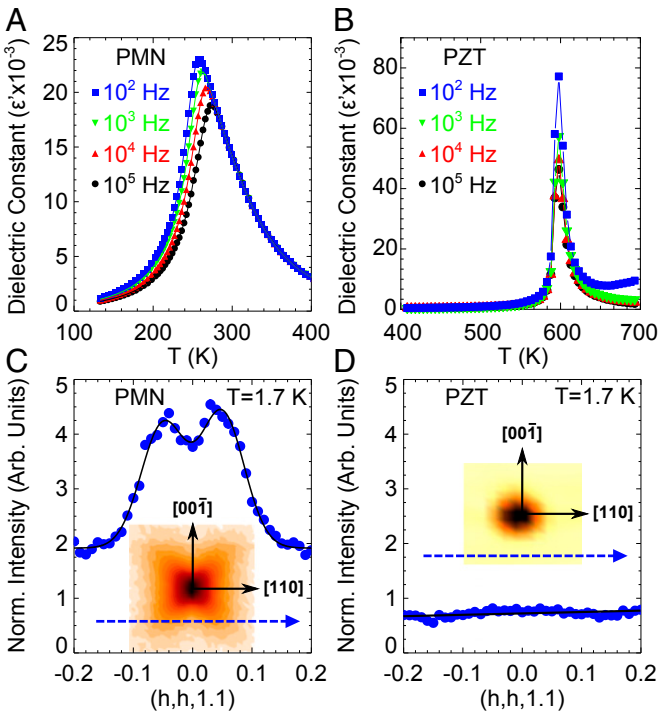

Fig. 1. Temperature dependence of the real part of the dielectric permittivity measured along [001] at 10^2, 10^3, 10^4, and 10^5 Hz for (*A*) PMN and (*B*) PZT ($x = 0.325$). Neutron elastic diffuse scattering intensity (solid blue dots) measured using the BT7 thermal-neutron spectrometer at 1.7 K along [110] in the (*HHL*) scattering plane for (*C*) PMN and (*D*) PZT. The strong, diffuse scattering peaks shown in *C* for PMN result from the large out-of-plane $\vec{Q}$ resolution, which overlaps with the four rods of diffuse scattering that point out of the (*HHL*) scattering plane and are centered at (001). These peaks are absent for PZT as shown in D. (*C, D*) *Insets* illustrate the shape of constant elastic-scattering-intensity contours measured near (001) in the (*HHL*) scattering plane for the same PMN and PZT crystals at 300 and 10 K, respectively, and are plotted on a log-intensity scale. Further details are provided in *SI Materials and Methods*.

shown in Fig. 1*B*, and no shift with temperature is evident. Instead the dielectric response of PZT is consistent with that of a conventional ferroelectric phase transition near 600 K. Thus, despite the many similarities between PZT and PMN, PZT is not a relaxor. This result is consistent with the theoretical work of Grinberg et al. who used density functional theory to parameterize a phenomenological Landau model of the dielectric frequency dispersion in terms of the average *B*-site cation displacement from the high-symmetry cubic structure, $\overline{D}_B$, and the second moment of the valence of the two *B*-site-cation nearest neighbors of each oxygen atom, $\langle V^2 \rangle$, which is a measure of the REF strength (15). Using only these two input parameters, the Grinberg model yields remarkable quantitative agreement with all of the 23 lead-based, perovskite relaxor systems for which both the local cation order and dielectric response have been measured. It is interesting to note that this model permits a frequency-dependent dielectric response even for materials where $\langle V^2 \rangle = 0$ (i.e., in the weak REF limit) provided that the average *B*-site cation displacement is not too large ($\overline{D}_B < 0.11$ Å). In the case of PZT, there is no frequency dependence because the average *B*-site cation displacement $\overline{D}_B$ is large enough (much larger than that in PMN) to stabilize long-range ferroelectric order. However, there exist other disordered perovskite materials composed of homovalent *B*-site cations for which $\langle V^2 \rangle = 0$ and $\overline{D}_B$ is small that do exhibit a strongly frequency-dependent dielectric response. Examples include compositions of BZT ($0.25 \leq x \leq 0.42$) and BST ($0.20 \leq x \leq 0.50$) (18), for which an average cubic symmetry is retained at all temperatures studied. Here we wish to consider the following fundamental questions: (*i*) are quenched REFs essential to the relaxor phase observed in the lead oxides; (*ii*) what is the relaxor-order parameter; (*iii*) is there a dynamical signature of the relaxor phase analogous to the soft mode that characterizes displacive ferroelectrics; and (*iv*) do REFs play a role in the ultrahigh piezoelectric response?

Results

Static Signature: Short-Range Polar Order. To answer these questions we compared the nanoscale structures of PMN and PZT using neutron-based measurements of the elastic diffuse scattering, which is arguably the single most interesting and intensely examined property of lead-oxide relaxors to date. Strong, temperature-dependent and highly anisotropic diffuse scattering has been documented in many different lead-oxide perovskite relaxors using X-ray and neutron-scattering methods (20–27). Fig. 1*C, Inset* illustrates the anisotropic nature of this diffuse scattering in PMN via a log-scale intensity map of the well-known, butterfly-shaped diffuse-scattering contours that decorate the (001) Bragg peak in the (*HHL*) scattering plane defined by the pseudocubic [110] and [001] crystallographic axes. We measured the diffuse-scattering intensity at very low temperature (1.7 K), where it is strongest, by scanning the neutron momentum transfer $\vec{Q}$ along the trajectory defined by the dashed blue arrow in Fig. 1*C*. These data are given by the solid blue dots, and two strong peaks are evident where this trajectory clips the two lower wings of the butterfly-shaped contours. The origin of this diffuse scattering is extremely controversial. Numerous models of the underlying short-range structural order have been proposed to explain the experimental data (25, 28–32). Neutron backscattering measurements (33, 34), which provide very sharp energy resolution ($\Delta E \sim 1$ μeV), show that truly elastic (i.e., static) diffuse scattering in PMN first appears at a temperature $T_d = 420 \pm 20$ K that coincides with that at which the lowest-frequency transverse optic (TO) phonon is softest and overdamped; it also grows monotonically on cooling (35). A monotonic increase of the diffuse scattering on cooling is observed in all pseudorhombohedral compositions of PMN-*x*PT and PZN-*x*PT (25, 36). Other neutron and X-ray studies have demonstrated that relaxor diffuse scattering is strongly affected by external electric fields (37, 38) and vanishes at high pressures (27, 39). For these reasons many researchers identify the diffuse scattering with static, nanometer-scale regions of short-range polar order known as polar nanoregions that condense from the soft TO mode on cooling from high temperatures well above T_{max} (23, 30). We emphasize that all lead-oxide perovskite relaxors for which single crystals have been examined with neutron or X-ray scattering techniques exhibit similar anisotropic, temperature-dependent diffuse-scattering contours including PMN, PZN, $Pb(Sc_{1/2}Nb_{1/2})O_3$, $Pb(Mg_{1/3}Ta_{2/3})O_3$, $Pb(In_{1/2}Nb_{1/2})O_3$, and $Pb(Sc_{1/2}Ta_{1/2})O_3$ (20, 22, 24–27, 30, 31). All of these compounds are composed of heterovalent *B*-site cations; hence $\langle V^2 \rangle > 0$. In addition, a recent neutron-scattering study discovered that the lead-free relaxor $(Na_{1/2}Bi_{1/2})TiO_3$ (NBT), an *A*-site disordered perovskite composed of heterovalent Na^+ and Bi^{3+} cations, displays static diffuse-scattering contours characterized by a temperature dependence and anisotropy like that found in PMN (40). This suggests that the physics that governs this diffuse scattering is not necessarily limited to lead-based perovskite relaxors.

By contrasting the elastic diffuse scattering from PMN to that from PZT, we can isolate the influence of quenched REFs on the nanometer-scale structure of lead-oxide perovskite relaxors. To this end we examined the neutron diffuse scattering from a single crystal of PZT with a Ti concentration $x = 0.325$ under exactly the same conditions as those used to measure the diffuse scattering from the PMN single crystal. To account precisely for differences in crystal size and beam illumination, the diffuse-scattering data from both crystals were normalized by the integrated intensity of a transverse acoustic (TA) phonon also measured under identical conditions. The resulting data, given by the solid blue dots in Fig. 1*D*, shows that the diffuse scattering for the nonrelaxor PZT is at least a factor of 20 weaker than that in PMN. Fig. 1*D, Inset*

shows a log-scale intensity map of the elastic scattering from the same PZT crystal at very low temperature (10 K) in the (HHL) scattering plane near (001), and no evidence of diffuse scattering is present. Additional data measured on PZT in the $(HK0)$ scattering plane at both low (16 K) and high (620 K) temperatures confirm this finding (Fig. S1). Static diffuse scattering was recently reported in a single crystal of PZT with $x = 0.475$ using X-ray inelastic scattering techniques (41). However, these data were obtained with an energy resolution nearly 10 times coarser than ours; hence there is a possibility of phonon contamination. This static diffuse scattering was modeled using a Huang formalism, which is inconsistent with that seen in relaxors, and was attributed to elastic deformations induced by defect centers of tetragonal symmetry. This is not unexpected for a composition so close to the MPB. Indeed such Huang scattering would have impaired our search for relaxor-like diffuse scattering except for the fact that our PZT composition $(x = 0.325)$ lies in the purely pseudorhombohedral regime.

As the only significant difference between PMN and PZT lies in the huge disparity in REF strength, our neutron data establish a direct causal link between strong REFs and the temperature-dependent, anisotropic diffuse scattering in lead-oxide perovskite relaxors. In the same vein, our dielectric permittivity measurements demonstrate that strong REFs are responsible for the relaxor-like behavior. Together these results imply the existence of a fundamental connection between the relaxor phase and the anisotropic, temperature-dependent diffuse scattering. We motivate this picture through a heuristic model, developed in the *SI Materials and Methods*, that allows us to relate the strength of the REFs to the diffuse-scattering intensity. We thus identify the relaxor-order parameter with the static, anisotropic diffuse scattering associated with short-range polar order, but only in the sense that it marks the transition temperature from the high-temperature paraelectric phase (where it is zero) to the low-temperature relaxor state (where it is nonzero). Indeed, as noted by Cowley et al. (13) and Prosandeev et al. (42) the strictly elastic diffuse scattering in PMN increases on cooling in a manner similar to that of an order parameter at a conventional phase transition, and this also holds true for all pseudorhombohedral compositions of PMN-xPT and PZN-xPT. As first discussed by Westphal et al. (10) and later Stock et al. (11), this identification is consistent with the ideas of Imry and Ma who showed that magnetic systems with continuous symmetry will break up into short-range ordered domains in the presence of random magnetic fields (43). In relaxors like PMN, long-range ferroelectric order is stifled by the formation of analogous polar domains on cooling. By contrast, our data show that no such domains form in ferroelectric PZT because the REFs are too weak. This picture naturally explains why the diffuse scattering in relaxors vanishes for compositions on the tetragonal side of the MPB; the uniaxial anisotropy there stabilizes the ferroelectric state.

Dynamic Signature: The Waterfall Effect Versus Zone-Boundary Soft Modes. We next compare the lattice dynamical properties of PZT and PMN to look for a dynamic signature of the relaxor phase. PMN exhibits several anomalous dynamical features that are also seen in other relaxor compounds such as PZN-xPT and $Pb(Mg_{1/3}Ta_{2/3})O_3$; thus the availability of a high-quality PZT single crystal provides us with a rare opportunity to determine if any of these are specific to lead-based perovskite relaxors. In particular, the diffuse scattering in PMN, which is purely relaxational above $T_d = 420$ K (44), has profound effects on the lifetimes of low-frequency TA modes (45, 46). The best-known dynamic anomaly is the "waterfall effect," a term coined to characterize the false impression that the soft TO phonon branch in PZN-8% PT drops steeply into the TA branch at a nonzero wave vector $|\vec{q}| \approx 0.2$ Å^{-1} (47). The waterfall effect results from a strong damping of the TO mode that occurs at significantly larger wave vectors than happens in cubic $PbTiO_3$ (48). The cause of this damping is also controversial. Model simulations based on standard TO–TA mode coupling theory provide qualitative agreement with experimental data measured on PZN-8%PT (49). However, TO–TA mode coupling has been shown to be weak in PMN and therefore unlikely to be the origin of the waterfall effect (45, 46). An alternative explanation is that the waterfall effect arises from disorder introduced through the heterovalent nature of the B-site cations, i.e., random dipolar fields (46). If this idea is correct, then the waterfall effect should be absent in PZT or qualitatively different from that observed in PMN and other relaxors. Another unusual dynamical feature is the simultaneous appearance of highly damped zone-boundary soft modes at the R- and M-point Brillouin zone boundaries in PMN (50), which exhibit a temperature dependence that tracks that of the soft, zone-center TO mode, and which give rise to broad superlattice peaks at the same locations. This behavior indicates that competing antiferroelectric and ferroelectric fluctuations are present in PMN, a situation that has been applied theoretically to $SrTiO_3$ (51). It was recently shown that the waterfall effect is present in PMN-60%PT, a composition that lies well beyond the MPB (52). Because PMN-60%PT exhibits no diffuse scattering and no discernable frequency dependence to the dielectric permittivity, the waterfall effect cannot be associated with the relaxor phase. The observation of a waterfall effect in PZT would provide additional evidence for this conclusion. By contrast, the soft and highly damped R- and M-point zone boundary modes seen in PMN are absent in PMN-60%PT (52) but have been observed in the relaxor PZN-5.5%PT; thus these broad modes may constitute a genuine dynamical signature of relaxors.

To determine if these dynamical anomalies are intrinsic to the relaxor state, we present neutron inelastic scattering data on PZT, which were obtained in the (HHL) scattering plane near the (220) Brillouin zone using a series of constant-$\vec{Q}$ and constant-$\hbar\omega$ scans. These scans probe TA and TO phonons polarized along [110] and propagating along [001], and they are directly comparable to those published on $PbTiO_3$ (48) and PZN-8%PT (47), all of which were measured in the same scattering plane and in the same Brillouin zone. The TA and TO phonon dispersion curves for PZT measured at 650 K (60 K above T_{C1}) are shown in Fig. 2*A*. We find that the TA phonon branch in PZT is similar to, but slightly softer than, the corresponding TA phonon branch in $PbTiO_3$, which is shown in Fig. 2*B* (48). The TO phonon branch in PZT drops to very low energies at small reduced-wave vectors $\vec{q} = \vec{Q} - (2, 2, 0)$ and is similar in this regard to the soft TO phonon branch in $PbTiO_3$ measured at 783 K (20 K above T_C). However, at large wave vectors the TO phonon branch in PZT is significantly softer than that in $PbTiO_3$ and closely resembles the TO phonon branch in the relaxor PZN-8%PT, which is also shown in Fig. 2*B*. In particular, the TO phonon branch in PZT

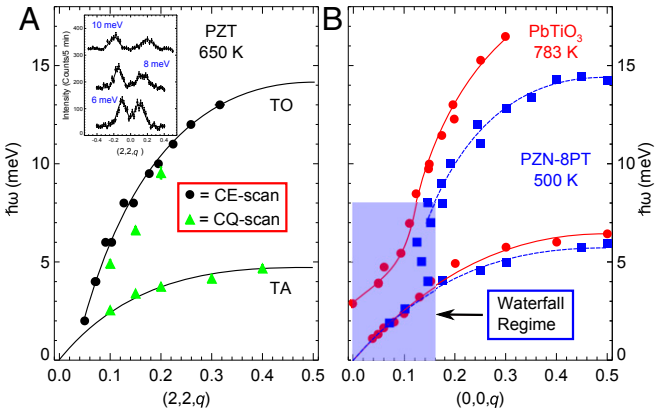

Fig. 2. Dispersions of the TA and soft TO modes measured in the (HHL) scattering plane near (220) in the cubic phases of (*A*) PZT and (*B*) $PbTiO_3$ (48) and PZN-8%PT (47). The green triangles/black circles in *A* denote the locations of maximum scattering intensity in constant-$\vec{Q}$/constant-$\hbar\omega$ scans, respectively; *Inset* shows constant-$\hbar\omega$ scans measured at 650 K at 6, 8, and 10 meV (data have been displaced vertically for clarity). All lines are guides to the eye.

appears to intercept the TA phonon branch at a nonzero wave vector near 0.05 reciprocal lattice units (rlu), albeit this is substantially smaller than the corresponding wave vector (0.14 rlu) in PZN-8%PT. This behavior suggests that the waterfall effect is present in PZT.

The nature of the waterfall effect in PZT is more fully revealed by an analysis of the constant-$\vec{Q}$ scans shown in Fig. 3 *A–D*, which were measured above and below the cubic-to-rhombohedral phase transition temperature $T_{C1} = 590$ K. The TO mode at $\vec{Q} = (2, 2, -0.2)$ is well-defined and softens on cooling from 900 to 650 K, but it is nearly overdamped at the same temperatures at $\vec{Q} = (2, 2, -0.1)$. In fact for wave vectors $|\vec{q}| < 0.15$ rlu, the TO mode is so damped that it is not possible to locate the peak in a constant-$\vec{Q}$ scan. This $\vec{q}$-dependent broadening of the soft TO mode is the hallmark of the waterfall effect and has been reported in various compositions of PMN-*x*PT and PZN-*x*PT. The solid lines in these panels represent fits of the data to the sum of two uncoupled damped harmonic oscillators convolved with the instrumental resolution function. The quality of the fits indicates that TA–TO mode coupling is weak in PZT for phonons propagating along [001]. A series of constant-$\vec{Q}$ scans were measured at $\vec{Q} = (2, 2, -0.15)$ between 300 and 900 K to characterize the temperature dependence of the TA phonon linewidth and energy. Fig. 3*E* shows that the TA phonon linewidth in PZT broadens on cooling from above T_{C1} and narrows slightly below. This behavior is markedly different from that in PMN (dashed lines) for which the TA phonon linewidth broadens enormously on cooling. The broadening in PMN has been shown to result from a coupling to a low-energy relaxational mode associated with the strong diffuse scattering (44, 45). Assuming that a coupling of similar strength is present in PZT, then the comparatively weak temperature-dependent TA phonon broadening would further support our finding of little or no diffuse scattering in this compound. In Fig. 3*F* the TA phonon energy in PZT is shown to vary monotonically and changes little with temperature. Indeed, the net shift in the PZT TA phonon energy over this broad temperature range is almost identical

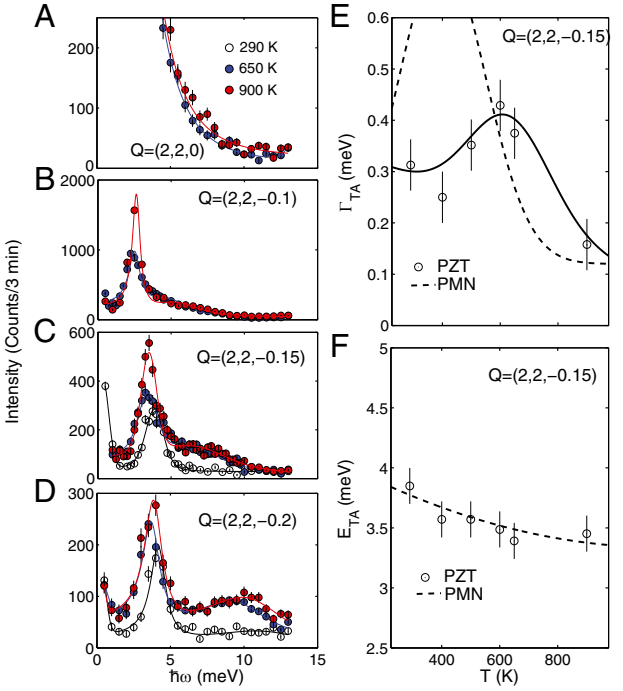

Fig. 3. Constant-$\vec{Q}$ scans measured at (*A*) (2,2,0), (*B*) (2,2,−0.1), (*C*) (2,2,−0.15), and (*D*) (2,2,−0.2) at temperatures above and below $T_{C1} = 590$ K. Temperature dependencies of the TA phonon (*E*) linewidth Γ_{TA} and (*F*) energy E_{TA} for PZT (open circles) and PMN (dashed lines). The solid line is a guide to the eye.

to that in PMN (dashed lines) (45, 46). We therefore exclude TA–TO mode coupling as the origin of the waterfall effect in PZT. We also exclude REFs as the mechanism responsible for the waterfall effect. At lower temperature (295 K), only the TA mode is visible because the TO mode has hardened to energies that lie outside the range of these scans. The softening of the TO mode on cooling from 900 to 650 K and the subsequent hardening is consistent with the cubic-to-rhombohedral phase transition at T_{C1} being driven by a soft, zone-center mode instability (53).

The lower-temperature phase transition for this composition of PZT at $T_{C2} = 370$ K corresponds to a doubling of the unit cell that is manifested by the appearance of new Bragg reflections at the R points $\left(\frac{h}{2}, \frac{\bar{h}}{2}, \frac{l}{2}\right)$, where h and l are odd and $h \neq l$. This suggests that there may be a soft mode at the R point. In PMN, highly damped (i.e., short-lived), soft zone-boundary modes are observed at both R and M points (Fig. S3), and structure-factor considerations preclude these from being octahedral tilt modes. To learn if PZT exhibits similar dynamics, we measured constant-$\vec{Q}$ scans at the R-point $\vec{Q} = \left(\frac{3}{2}, \frac{3}{2}, -\frac{1}{2}\right)$ at 290, 650, and 900 K, which are shown in Fig. 4*A*, *Upper*. A broad distribution of scattering is observed in PZT below 10 meV at 900 and 650 K but is absent at 290 K. The shift in spectral weight from high to low energies on cooling from 900 K is particularly apparent near $\hbar\omega = 2.0$ meV where an increase in scattering is seen at 290 K. To clarify this behavior we measured the scattering intensity at $\vec{Q} = \left(\frac{3}{2}, \frac{3}{2}, -\frac{1}{2}\right)$ and $\hbar\omega = 2.0$ meV as a function of temperature. The data (Fig. 4*A*, *Lower*) show that the scattering at 2 meV increases on cooling from 900 K to a maximum at near 450 K and then decreases. This behavior is precisely that expected for a soft mode: for $T > T_{C2}$ the soft mode is located above 2 meV, which results in little or no scattering; but on cooling through T_{C2} the soft mode drops to lower energies, thus moving into and then out of the instrumental window and causing the scattering intensity to first increase and then decrease. This procedure mimics that used by Swainson et al. to demonstrate the softening of the R-point zone-boundary mode in PMN (50).

We performed identical measurements on PZT at the M points $\left(\frac{3}{2}, \frac{3}{2}, 0\right)$ and $\left(\frac{3}{2}, \frac{3}{2}, 1\right)$ at the same energy transfer $\hbar\omega = 2.0$ meV. These data, shown in Fig. 4*B*, *Upper*, reveal completely different behavior as comparatively little temperature dependence is observed. This is consistent with the fact that no superlattice reflections are seen at M-point locations in this composition of PZT (53). It also points to a fundamental difference in the dynamics between PZT and PMN for which concurrent, broad, soft zone-boundary modes were observed at both R and M points as indicated in Fig. 4*B*, *Lower*. At higher Ti concentrations ($x = 0.475$) PZT exhibits a low-temperature monoclinic phase, and X-ray inelastic measurements have observed soft M-point modes (54). However, no soft R-point mode was reported for this monoclinic composition. We thus propose that a competition between ferroelectric and antiferroelectric fluctuations, as revealed by the simultaneous presence of heavily damped (short-lived) soft modes at the R, M, and Γ points, may represent a true dynamical signature of relaxor behavior.

Ultrahigh Piezoelectricity. It is well known that pseudorhombohedral compositions of PMN-*x*PT and PZN-*x*PT located near the MPB exhibit enormous piezoelectric coefficients; the values of the longitudinal piezoelectric coefficient d_{33} for single-crystal MPB compositions of PMN-*x*PT and PZN-*x*PT poled along [001] can exceed 2,800 pC/N and are the largest known (6, 55, 56). The concepts of polarization rotation (2) and adaptive phases (3) were proposed to explain the ultrahigh electromechanical response in MPB systems like PZT and PMN-*x*PT. More recently, Kutnjak et al. reported that the origin of the giant electromechanical response at the MPB is related to the proximity of the system to a critical end point (4). We note here that the *q*-integrated neutron elastic diffuse-scattering intensity in PMN-*x*PT, which from the fluctuation-dissipation theorem is a measure of the static susceptibility, and d_{33} share a similar composition dependence

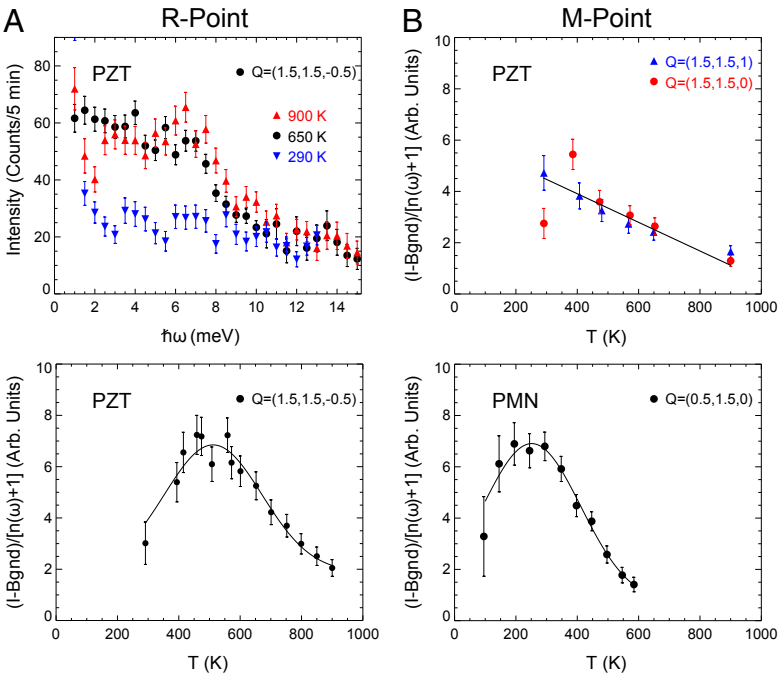

Fig. 4. (*A, Upper*) Constant-$\vec{Q}$ scans measured at the R point $(\frac{3}{2},\frac{3}{2},-\frac{1}{2})$ at 900, 650, and 290 K. (*Lower*) Background subtracted intensity, adjusted by the Bose factor $[n(\omega)+1]$, measured at the same $\vec{Q}$ and at fixed $\hbar\omega = 2.0$ meV from 900 to 300 K. (*B, Upper*) Neutron-scattering intensity measured at the M points $(\frac{3}{2},\frac{3}{2},0)$ (solid red circles) and $(\frac{3}{2},\frac{3}{2},1)$ (solid blue triangles) from 900 to 300 K. The background has been subtracted from the total scattering intensity and the result adjusted by the Bose factor $[n(\omega)+1]$. (*Lower*) Analogous data for the relaxor PMN measured by Swainson et al. (50) at $\vec{Q} = (\frac{3}{2},\frac{3}{2},0)$.

(36, 57). Both properties (in this case measured along [110]) peak near the MPB and then decrease precipitously in the tetragonal (Ti rich) regime in which the relaxor phase is replaced by a conventional ferroelectric phase (52). Given our finding that PZT exhibits essentially no such diffuse scattering one might expect that the corresponding value of d_{33} in PZT should be significantly smaller than that in PMN-xPT. We find that this is indeed true: the value of d_{33} that we measured on a [001]-poled single crystal of PZT with a composition close to the MPB is 1,200 pC/N. Thus, the optimal values of d_{33} in single-crystal PMN-xPT and PZN-xPT are ~100% greater than that in single-crystal PZT. Insofar as PZT and PMN-xPT are identical systems save for the strength of the REFs, our results indicate that the underlying nanometer-scale, static, polar order in relaxors that is associated with the temperature-dependent diffuse scattering plays a seminal role in greatly amplifying the piezoelectric response beyond that in the nonrelaxor PZT, which does not display an equivalent nanometer-scale polar order. This conclusion is consistent with the theoretical results of Pirc et al. that suggest polar nanoregions play an important role in the electrostriction in relaxors (58). Kutnjak et al. also showed that the phase transitions in relaxor-based ferroelectrics are first order as an external electric field must be applied to reach the critical end point. By contrast, PZT compositions near the MPB exhibit second-order phase transitions (critical points) at T_C in zero field (59). This suggests that the presence of REFs is at least as important to the large piezoelectric response as is the proximity of the system to a critical end point. We note that this behavior is not without precedent. In single crystals of highly magnetostrictive galfenol, an alloy of magnetic Fe and nonmagnetic Ga that is often likened to a magnetic relaxor and which should possess strong random magnetic fields, both the neutron elastic diffuse scattering intensity and the longitudinal magnetostrictive coefficient λ_{100} increase dramatically as the system is doped toward a phase boundary and then decrease sharply as the boundary is crossed (60).

Conclusions

We have performed a detailed comparison of the dielectric permittivity, nanoscale structure, and lattice dynamics of two highly similar, disordered, lead-oxide perovskite compounds that correspond to the limits of weak (PZT) and strong (PMN) random electric fields. The relative weakness (or absence) of any elastic, anisotropic, and temperature-dependent diffuse scattering in PZT of the type observed in the relaxor PMN proves that the static, short-range polar displacements found in the lead-oxide perovskite relaxors are not prevalent in ferroelectric PZT and therefore require the presence of strong REFs. The lack of any frequency dispersion in the dielectric permittivity of PZT further indicates that the relaxor phase in these lead-oxide perovskites also requires the presence of strong REFs. These conclusions have fundamental ramifications for the definition of the relaxor state because they imply that perovskite relaxors with homovalent B-site disorder such as BZT and BST do not belong in the same classification as the lead-oxide perovskite relaxors, even though these systems all exhibit frequency-dependent dielectric susceptibilities. Because the corresponding REFs in such homovalent compounds are weak in comparison with any crystalline anisotropy energy, the frequency dependence of the dielectric permittivity must have a different physical origin. Moreover, none of these homovalent compounds has been shown to exhibit the elastic, anisotropic, and temperature-dependent diffuse scattering seen in the lead-based relaxors (40), which we show boosts the piezoelectricity to record-setting levels. In the cases of BZT and BST, as well as many other $BaTiO_3$-based "relaxors," only temperature-independent, sheetlike diffuse scattering, similar to that seen in paraelectric $BaTiO_3$, has been observed using electron-diffraction methods (18). We hope that our results will motivate further experimental and theoretical studies of relaxors, which are essential to clarify the physics of random electric fields in condensed matter systems.

ACKNOWLEDGMENTS. The authors acknowledge fruitful discussions with R. E. Erwin, D. K. Singh, and L. Kneller regarding the use and fabrication of a single-crystal silicon sample mount. This work used facilities supported in part by the National Science Foundation under Agreement DMR-0944772. The work at Simon Fraser University was supported by the US Office of Naval Research (Grants N00014-11-1-0552 and N00014-12-1-1045) and the Natural Science and Engineering Research Council of Canada. C.S. was partially supported by the Carnegie Trust. P.G. was supported by the Center for Nanophase Materials Sciences, which is sponsored at Oak Ridge National Laboratory by the Scientific User Facilities Division, Office of Basic Energy Sciences, US Department of Energy.

1. Bellaiche L, Vanderbilt D (1999) Intrinsic piezoelectric response in perovskite alloys: PMN-PT versus PZT. *Phys Rev Lett* 83:1347–1350.
2. Fu H, Cohen RE (2000) Polarization rotation mechanism for ultrahigh electromechanical response in single-crystal piezoelectrics. *Nature* 403(6767):281–283.
3. Jin YM, Wang YU, Khachaturyan AG, Li JF, Viehland D (2003) Conformal miniaturization of domains with low domain-wall energy: Monoclinic ferroelectric states near the morphotropic phase boundaries. *Phys Rev Lett* 91(19):197601.
4. Kutnjak Z, Petzelt J, Blinc R (2006) The giant electromechanical response in ferroelectric relaxors as a critical phenomenon. *Nature* 441(7096):956–959.
5. Xu G, Wen J, Stock C, Gehring PM (2008) Phase instability induced by polar nanoregions in a relaxor ferroelectric system. *Nat Mater* 7(7):562–566.
6. Park SE, Shrout TR (1997) Ultrahigh strain and piezoelectric behavior in relaxor based ferroelectric single crystals. *J Appl Phys* 82(4):1804.
7. Uchino K (1996) *Piezoelectric Actuators and Ultrasonic Motors* (Kluwer Academic, Boston).
8. Kandilian R, Navid A, Pilon L (2011) The pyroelectric energy harvesting capabilities of PMN-PT near the morphotropic phase boundary. *Smart Mater Struct* 20(5):055020.
9. Vugmeister BE, Glinchuk MD (1990) Dipole glass and ferroelectricity in random-site electric dipole systems. *Rev Mod Phys* 62(4):993–1026.
10. Westphal V, Kleeman W, Glinchuk MD (1992) Diffuse phase transitions and random-field-induced domain states of the "relaxor" ferroelectric $PbMg_{1/3}Nb_{2/3}O_3$. *Phys Rev Lett* 68(6):847–850.
11. Stock C, et al. (2004) Universal static and dynamic properties of the structural transition in $Pb(Zn_{1/3}Nb_{2/3})O_3$. *Phys Rev B* 69(9):094104.
12. Tinte S, Burton B, Cockayne E, Waghmare U (2006) Origin of the relaxor state in $Pb(B_xB'_{1-x})O_3$ perovskites. *Phys Rev Lett* 97(13):137601.
13. Cowley RA, Gvasaliya SN, Lushnikov SG, Roessli B, Rotaru GM (2011) Relaxing with relaxors: A review of relaxor ferroelectrics. *Adv Phys* 60(2):229–327.
14. Pirc R, Blinc R (1999) Spherical random-bond-random-field model of relaxor ferroelectrics. *Phys Rev B* 60(19):13470–13478.
15. Grinberg I, Juhás P, Davies PK, Rappe AM (2007) Relationship between local structure and relaxor behavior in perovskite oxides. *Phys Rev Lett* 99(26):267603.
16. Akbarzadeh AR, Prosandeev S, Walter EJ, Al-Barakaty A, Bellaiche L (2012) Finite-temperature properties of $Ba(Zr,Ti)O_3$ relaxors from first principles. *Phys Rev Lett* 108(25):257601.
17. Samara SA (2003) The relaxational properties of compositionally disordered ABO_3 perovskites. *J Phys Condens Matter* 15(9):R367–R411.
18. Liu Y, Withers RL, Nguyen B, Elliott K (2007) Structurally frustrated polar nanoregions in $BaTiO_3$-based relaxor ferroelectric systems. *Appl Phys Lett* 91(15):152907.
19. Bokov AA, Long X, Ye ZG (2010) Optically isotropic and monoclinic ferroelectric phases in $Pb(Zr_{1-x}Ti_x)O_3$ (PZT) single crystals near morphotropic phase boundary. *Phys Rev B* 81(17):172103.
20. Vakhrushev SB, Naberezhnov AA, Okuneva NM, Savenko BN (1995) Determination of polarization vectors in lead magnoniobate. *Phys Solid State* 37(12):1993–1997.
21. You H, Zhang QM (1997) Diffuse X-ray scattering study of lead magnesium niobate single crystals. *Phys Rev Lett* 79(20):3950–3953.
22. Malibert C, et al. (1997) Order and disorder in the relaxor ferroelectric perovskite $PbSc_{1/2}Nb_{1/2}O_3$ (PSN): comparison with simple perovskites $BaTiO_3$ and $PbTiO_3$. *J Phys Condens Matter* 9(35):7485–7500.
23. Hirota K, Ye ZG, Wakimoto S, Gehring PM, Shirane G (2002) Neutron diffuse scattering from polar nanoregions in the relaxor $Pb(Mg_{1/3}Nb_{2/3})O_3$. *Phys Rev B* 65(10):104105.
24. Gvasaliya SN, Roessli B, Lushnikov SG (2003) Neutron diffuse scattering from $PbMg_{1/3}Ta_{2/3}O_3$ relaxor ferroelectric. *Europhys Lett* 63(2):303–309.
25. Xu G, Zhong Z, Hiraka H, Shirane G (2004) Three-dimensional mapping of diffuse scattering in $Pb(Zn_{1/3}Nb_{2/3}O_3$-$xPbTiO_3$. *Phys Rev B* 70(17):174109.
26. Ohwada K, Hirota K, Terauchi H, Ohwa H, Yasuda N (2006) Spatial distribution of the B-site inhomogeneity in an as-grown $Pb(In_{1/2}Nb_{1/2})O_3$ single crystal studied by a complementary use of X-ray and neutron scatterings. *J Phys Soc Jpn* 75(2):024606.
27. Mihailova B, et al. (2008) Pressure-induced phase transition in $PbSc_{0.5}Ta_{0.5}O_3$ as a model Pb-based perovskite-type relaxor ferroelectric. *Phys Rev Lett* 101(1):017602.
28. Welberry TR, Goossens DJ, Gutmann MJ (2006) Chemical origin of nanoscale polar domains in $PbZn_{1/3}Nb_{2/3}O_3$. *Phys Rev B* 74(22):224108.
29. Paściak M, Wocyrz M, Pietraszko A (2007) Interpretation of the diffuse scattering in Pb-based relaxor ferroelectrics in terms of three-dimensional nanodomains of the 110-directed relative interdomain atomic shifts. *Phys Rev B* 76(1):014117.
30. Ganesh P, et al. (2010) Origin of diffuse scattering in relaxor ferroelectrics. *Phys Rev B* 81(14):144102.
31. Cervellino A, et al. (2011) Diffuse scattering from the lead-based relaxor ferroelectric $PbMg_{1/3}Ta_{2/3}O_3$. *J Appl Cryst* 44(3):603–609.
32. Bosak A, Chernyshov D, Vakhrushev S, Krisch M (2012) Diffuse scattering in relaxor ferroelectrics: True three-dimensional mapping, experimental artefacts and modelling. *Acta Crystallogr A* 68(1):117–123.
33. Gehring PM, Neumann DA (1998) Backscattering spectroscopy at the NIST Center for Neutron Research. *Physica B* 241–243:64–70.
34. Meyer A, Dimeo RM, Gehring PM, Neumann DA (2003) The high-flux backscattering spectrometer at the NIST Center for Neutron Research. *Rev Sci Instrum* 74(5):2759–2777.
35. Gehring PM, et al. (2009) Reassessment of the Burns temperature and its relationship to the diffuse scattering, lattice dynamics, and thermal expansion in relaxor $Pb(Mg_{1/3}Nb_{2/3})O_3$. *Phys Rev B* 79(22):224109.
36. Matsuura M, et al. (2006) Composition dependence of the diffuse scattering in the relaxor ferroelectric compound (1-x)$Pb(Mg_{1/3}Nb_{2/3})O_3$-$xPbTiO_3$($0 \le x \le 0.40$). *Phys Rev B* 74(14):144107.
37. Gehring PM, Ohwada K, Shirane G (2004) Electric-field effects on the diffuse scattering in $PbZn_{1/3}Nb_{2/3}O_3$ doped with 8% $PbTiO_3$. *Phys Rev B* 70(1):014110.
38. Stock C, et al. (2007) Neutron and x-ray diffraction study of cubic [111] field-cooled $Pb(Mg_{1/3}Nb_{2/3})O_3$. *Phys Rev B* 76(6):064122.
39. Chaabane B, Kreisel J, Dkhil B, Bouvier P, Mezouar M (2003) Pressure-induced suppression of the diffuse scattering in the model relaxor ferroelectric $PbMg_{1/3}Nb_{2/3}O_3$. *Phys Rev Lett* 90(25):257601.
40. Ge W, et al. (2013) Lead-free and lead-based ABO_3 perovskite relaxors with mixed-valence A-site and B-site disorder: Comparative neutron scattering structural study of $(Na_{1/2}Bi_{1/2})TiO_3$ and $Pb(Mg_{1/3}Nb_{2/3})O_3$. *Phys Rev B* 88(17):174115.
41. Burkovsky RG, et al. (2012) Structural heterogeneity and diffuse scattering in morphotropic lead zirconate-titanate single crystals. *Phys Rev Lett* 109(9):097603.
42. Prosandeev S, et al. (2013) Condensation of the atomic relaxation vibrations in lead-magnesium-niobate at T=T*. *J Appl Phys* 114(12):124103.
43. Imry Y, Ma SK (1975) Random-field instability of the ordered state of continuous symmetry. *Phys Rev Lett* 35(21):1399–1401.
44. Stock C, et al. (2010) Interplay between static and dynamic polar correlations in relaxor $Pb(Mg_{1/3}Nb_{2/3})O_3$. *Phys Rev B* 81(14):144127.
45. Stock C, et al. (2005) Strong influence of the diffuse component on the lattice dynamics in $Pb(Mg_{1/3}Nb_{2/3})O_3$. *J Phys Soc Jpn* 74(11):3002–3010.
46. Stock C, et al. (2012) Evidence for anisotropic polar nanoregions in relaxor $Pb(Mg_{1/3}Nb_{2/3})O_3$: A neutron study of the elastic constants and anomalous TA phonon damping in PMN. *Phys Rev B* 86(10):104108.
47. Gehring PM, Park SE, Shirane G (2000) Soft phonon anomalies in the relaxor ferroelectric $Pb[(Zn_{1/3}Nb_{2/3})_{0.92}Ti_{0.08}]O_3$. *Phys Rev Lett* 84(22):5216–5219.
48. Shirane G, Axe JD, Harada J, Remeika JP (1970) Soft ferroelectric modes in lead titanate. *Phys Rev B* 2(1):155–159.
49. Hlinka J, et al. (2003) Origin of the waterfall effect in phonon dispersion of relaxor perovskites. *Phys Rev Lett* 91(10):107602.
50. Swainson IP, et al. (2009) Soft phonon columns on the edge of the Brillouin zone in the relaxor $PbMg_{1/3}Nb_{2/3}O_3$. *Phys Rev B* 79(22):224301.
51. Zhong W, Vanderbilt D (1995) Competing structural instabilities in cubic perovskites. *Phys Rev Lett* 74(13):2587–2590.
52. Stock C, et al. (2006) Damped soft phonons and diffuse scattering in 40%$Pb(Mg_{1/3}Nb_{2/3})O_3$-60%$PbTiO_3$. *Phys Rev B* 73(6):064107.
53. Phelan D, et al. (2010) Single crystal study of competing rhombohedral and monoclinic order in lead zirconate titanate. *Phys Rev Lett* 105(20):207601.
54. Hlinka J, et al. (2011) Soft antiferroelectric fluctuations in morphotropic $PbZr_{1-x}Ti_xO_3$ single crystals as evidenced by inelastic x-ray scattering. *Phys Rev B* 83(14):140101.
55. Guo Y, et al. (2003) The phase transition sequence and the location of the morphotropic phase boundary region in (1-x)$[PbMg_{1/3}Nb_{2/3}O_3]$-$xPbTiO_3$ single crystal. *J Phys Condens Matter* 15(2):L77–L82.
56. Cao H, Schmidt VH, Zhang R, Cao W, Luo H (2004) Elastic, piezoelectric, and dielectric properties of 0.58$Pb(Mg_{1/3}Nb_{2/3})O_3$-0.42$PbTiO_3$ single crystal. *J Appl Phys* 96(1):549–554.
57. Gehring PM (2012) Neutron diffuse scattering in lead-based relaxor ferroelectrics and its relationship to the ultra-high piezoelectricity. *J Adv Dielectr* 2(2):1241005.
58. Pirc R, Blinc R, Vikhnin V (2004) Effect of polar nanoregions on giant electrostriction and piezoelectricity in relaxor ferroelectrics. *Phys Rev B* 69(21):212105.
59. Kim T, Ko JH, Kojima S, Bokov A, Ye ZG (2012) Phase transition behaviors of $PbZr_{1-x}Ti_xO_3$ single crystals as revealed by elastic anomalies and central peaks. *Appl Phys Lett* 100(8):082903.
60. Cao H, et al. (2009) Role of nanoscale precipitates on the enhanced magnetostriction of heat-treated galfenol ($Fe_{1-x}Ga_x$). *Phys Rev Lett* 102(12):127201.